Scientific Research Publishing

Journal of Water Resource and Protection, 2026, 18(11), 793-811
https://www.scirp.org/journal/jwarp
ISSN Online: 1945-3108
ISSN Print: 1945-3094

# Historical Evolution of Flooding in Abidjan (1960-2026): Trend Analysis and the Role of Rainfall

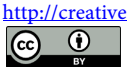
**Kan Martin Kouassi, N'Diaye Hermann Meledje**

Research Center for Ecology, Nangui Abrogoua University, Abidjan, Côte d'Ivoire
Email: kanstephane@gmail.com

**How to cite this paper:** Kouassi, K.M. and Meledje, N.H. (2026) Historical Evolution of Flooding in Abidjan (1960-2026): Trend Analysis and the Role of Rainfall. *Journal of Water Resource and Protection*, **18**, 793-811.
https://doi.org/10.4236/jwarp.2026.1811039

**Received:** September 28, 2026
**Accepted:** November 16, 2026
**Published:** November 19, 2026

Copyright © 2026 by author(s) and Scientific Research Publishing Inc.
This work is licensed under the Creative Commons Attribution International License (CC BY 4.0).
http://creativecommons.org/licenses/by/4.0/



Open Access

## Abstract

This study analyzes the floods recurrence (1960-2026), identifies the most affected areas, and examines the precipitation role. It is based on flood data and annual death tolls (1960-June 2026) provided by the National Office of Civil Protection (ONPC) and the press, as well as daily rainfall data from the ERA5 reanalysis (1960-2025) and the ORIESA network (2015-2023). The temporal and spatial variability of floods and the influence of rainfall on mortality were analyzed using GIS and statistical tests. The results identified 27 floods over 20 years. The number of episodes per decade increased by a factor of 1.8 (Poisson regression, $p < 0.001$). Deaths per million inhabitants per year rose from 1.19 in the 1990s to 2.12 in 2020-2026. Over 1960-2025, annual maximum 1-day (Rx1day) and 3-day (Rx3day) rainfall increased (+0.37 and +0.41 mm/year), while total annual rainfall (PRCPTOT) decreased (−7.2 mm/year). Neither the annual extremes nor ERA5 rainfall on flood days showed a significant correlation with death tolls. However, ORIESA data show that ERA5 substantially underestimates the thunderstorms that trigger flooding: six of eight events exceeded 100 mm at one or more rain gauges (up to 329.3 mm), compared with at most 86.8 mm in ERA5. Attécoubé, Cocody, Yopougon, and Abobo are the most affected municipalities. Flooding in Abidjan is triggered by intense, highly localized thunderstorms, while the human toll is plausibly linked to the exposure and vulnerability of the affected areas.

## Keywords

Abidjan, Côte d'Ivoire, Urban Flooding, Flood-Related Mortality, Extreme Rainfall, ERA5, Urban Vulnerability

## 1. Introduction

Over the past few decades, episodes of extreme rainfall have come to be regarded as natural disasters in West African cities, with a growing socioeconomic impact [1] [2].

Various approaches can be used to characterize the extreme nature of these rainfall events. Statistical methods assign a return period to each rainfall event to determine its exceptional nature [3] [4]. Other studies combine several characteristics of watersheds within a geographic information system (GIS) to map areas at risk [5]-[7]. However, in the current context of climate change and increasing urbanization, where the assumption of climate stationarity is being challenged, an approach that considers loss of life, property damage, or environmental disruption to characterize the extreme or exceptional nature of a rainfall event appears more relevant.

This study, which analyzes the flood history of the Autonomous District of Abidjan, fits within this context. This metropolis, which is expanding both demographically and spatially, has been facing recurrent flooding for several decades, with increasing socioeconomic and environmental impacts. Despite the stormwater mitigation and management measures implemented by the authorities, flooding has become a nearly annual occurrence, revealing the structural vulnerability of Abidjan's urban system to hydroclimatic hazards [8]. This research aims to characterize and analyze the dynamics of historical floods and extreme rainfall in the Abidjan district to better understand the role of precipitation in the recurrence of floods from 1960 to 2026. More specifically, the objectives are to:

- analyze the temporal variability of past extreme events in the Abidjan district to assess their recurrence, intensity, evolution over time, and the vulnerability of the urban landscape;
- highlight the relationship between the occurrence of extreme rainfall and the evolution of floods and their human impacts within Abidjan's urban fabric.

## 2. Study Area

The Abidjan District extends approximately between 5˚03' and 5˚39' north latitude and between 4˚33' and 3˚39' west longitude, in southeastern Côte d'Ivoire (**Figure 1**). It comprises the thirteen municipalities of the Autonomous District of Abidjan: Abobo, Adjamé, Anyama, Attécoubé, Bingerville, Cocody, Koumassi, Marcory, Le Plateau, Port-Bouët, Songon, Treichville, Brofodoumé and Yopougon, distributed around the Ébrié Lagoon. This coastal metropolis features generally low-lying terrain (0 to 146 m), a dense river network, and a high rate of land development. The combination of these physical characteristics with rapid urbanization, soil sealing, and inadequate drainage significantly increases its vulnerability to urban flooding [1].

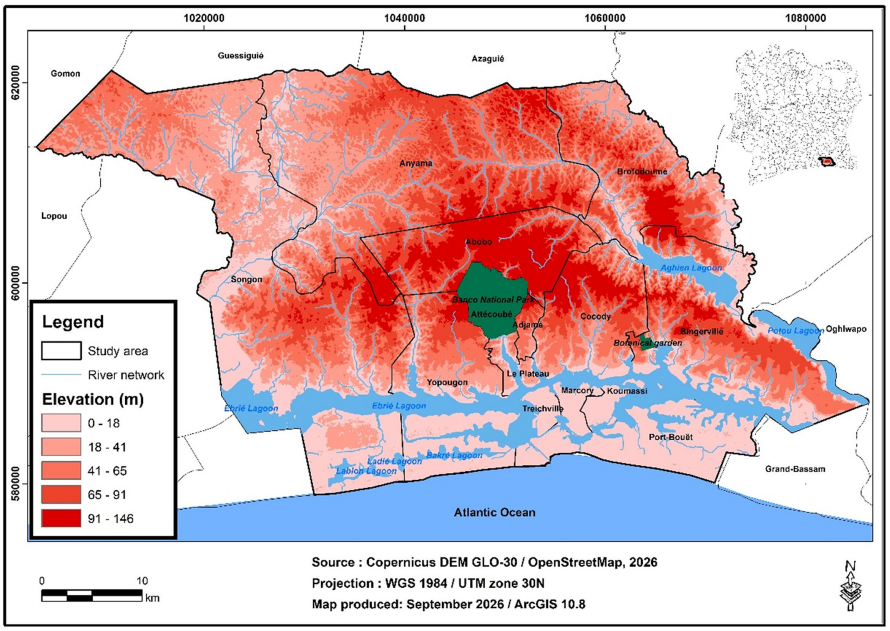



Figure 1. Location and topography of the Abidjan District.

## 3. Materials and Methods

### 3.1. Data Sources and Compilation

The data used in this study are:

- A historical record of reported floods, whether they caused damage. These data are derived from compilations of official reports from the National Office for Civil Protection (ONPC), as reported by the Ivorian press (Abidjan.net, Fraternité Matin, AIP), from 1960 to June 2026. For each year, the number of floods, their dates, and the cumulative annual death toll were recorded. A flood episode or episode is defined as any reported flood in the Abidjan district, whether or not it caused deaths. For the oldest events, the inventory relies mainly on Fraternité Matin; for recent events, it combines Fraternité Matin and ONPC reports. When several sources reported the same event, or when their death tolls differed, priority was given to government or government-affiliated sources (ONPC, Fraternité Matin). Years for which no report was found were counted as years without a recorded flood; this reflects an absence of documentation rather than a confirmed absence of flooding or deaths.
- Daily precipitation from the ERA5 reanalysis [9], extracted via the Open-Meteo archive for the grid point closest to Abidjan Airport (5.25˚N; 3.93˚W), from January 1, 1960, to August 20, 2026. These data were used to calculate annual rainfall indices, namely maximum daily rainfall (Rx1day), maximum cumulative rainfall over 3 and 5 consecutive days (Rx3day, Rx5day), and annual cumulative rainfall (PRCPTOT), as well as the rainfall associated with each dated flood event. The ERA5 dataset was selected because it is the only daily rainfall series available for Abidjan that is both complete and homogeneous for the period 1960-2026. It contains no missing days and is produced using the same

assimilation system throughout the entire period, whereas the airport station series (SODEXAM) is highly incomplete and may exhibit gaps due to changes in instruments or observation practices. These characteristics make it suitable for analyzing long-term trends and the regional rainfall regime, but not for estimating the intensity of individual convective thunderstorms. Since ERA5 smooths out local convective rainfall at its 0.25˚ resolution, these indices are interpreted as indicators of the regional rainfall regime rather than as point-specific intensities. Since the year 2026 is incomplete, its annual indices were excluded from the trend analyses.

- Daily observations from the Abidjan Airport station (WMO 65578), obtained via the Meteostat archive. The series begins in 1973 but is highly incomplete; only the years 2023, 2024, and 2025 have more than 95% of days with recorded data, and these three years were used to evaluate ERA5.
- Daily rainfall data from the ORIESA network of tipping-bucket rain gauges [10], 20 of which are in the Abidjan district, available from February 2015 to June 2023. Values flagged as questionable by the data providers were excluded.
- The population for each flood year, provided by the National Institute of Statistics (INS), to estimate the number of deaths per million inhabitants [11].

## 3.2. Methodology

### 3.2.1. Temporal and Spatial Analysis of Floods

The temporal analysis involved counting the number of episodes each year, noting that a single year could have multiple episodes. The counts were grouped by decade. The months in which the events occurred were identified to determine seasonality over the period 1960-2026. The trend in the annual number of episodes was tested using a Poisson regression on the year; the multiplicative variation by decade was calculated as $\exp(10\beta)$, and overdispersion was assessed using Pearson's dispersion statistic. To account for improvements in flood data collection, the regression was repeated for the period 1996-2026. The proportion of years with at least one event before 2014 and since 2014 was compared using Fisher's exact test.

The spatial dimension was analyzed in a geographic information system based on the location of events by municipality. Since a single flood can affect multiple municipalities, each event was counted once in each of the affected municipalities. The number of episodes per municipality, its share of the total number of episodes, and the spatial extent of each episode (number of affected municipalities) were calculated. These indicators were then mapped to identify areas with the highest concentration of events and the most widespread events.

### 3.2.2. Assessment of the Human Impacts of Floods

Human impacts were assessed based on the annual number of deaths, also relative to the interpolated population between the census of 1975, 1988, 1998, 2014, and 2021 [11]. The cumulative number of deaths was calculated for each decade. Given the large number of years with no deaths and the asymmetric distribution of

deaths, trends were examined primarily using medians, frequencies, and Spearman's rank correlation between the year and the number of deaths.

#### 3.2.3. Influence of Extreme Precipitation on Flooding

The influence of precipitation on mortality was studied for years with flooding, using correlations between the number of deaths and the Rx1day, Rx3day, Rx5day, and PRCPTOT indices. Spearman's correlation was chosen as the primary method due to the small sample size, the asymmetry of the death distribution, and the possible presence of outliers. The indices for years with and without flooding were compared using Welch's t-test and the Mann-Whitney U test. Given the small sample size, 95% confidence intervals for $\rho$ were calculated using Fisher's z-transformation, and the minimum detectable correlation with 80% power at the 5% significance level ($|\rho| \approx 0.59$) is reported. A 5% significance level was used for all tests.

Trends in precipitation indices were assessed from 1960 to 2025 using the Mann-Kendall test [12] [13] combined with Sen's slope [14]. Autocorrelation was assessed using the first-order autocorrelation coefficient; when it was significant (PRCPTOT), the test was repeated after trend-free pre-whitening (TFPW) [15].

For each precisely dated event, ERA5 precipitation data were extracted for the flood day(s) (P1d) and for the 3- and 5-day periods ending on each flood day (P3d, P5d), using the maximum value over the event. Return periods were estimated using a Gumbel distribution fitted by the method of moments to the annual maxima from 1960 to 2025 of the same duration [4]. For years with multiple episodes, the heaviest event rainfall was correlated with the annual death toll using Spearman's rank correlation test. Finally, the ERA5 data set was compared with the airport station on the days of the station's annual maxima in 2023-2025.

The ORIESA network was used to measure rainfall associated with the dated floods it covers, using the maximum daily rainfall at each rain gauge on the flood day(s) and the preceding day to account for nighttime thunderstorms and the division of days according to Greenwich Mean Time (GMT), and to evaluate ERA5 over the 2015-2023 period by comparing ERA5 daily values to the network's average and maximum on days when at least three rain gauges were operational. Isolated rainfall events were compared to the distribution of annual maximum values from the rain gauges. The spatial consistency of rainfall was described by the daily correlation between pairs of rain gauges as a function of distance.

## 4. Results

### 4.1. Frequency of Floods between 1960 and 2026

Between 1960 and 2026, 27 floods were recorded over 20 years (**Figure 2**). Before 2014, events were mostly isolated, with two sequences of consecutive years (1996-1998 and 2007-2010). Since 2014, floods have been reported in 10 of 13 years, and years with multiple episodes have become more frequent, reaching four episodes in 2022.

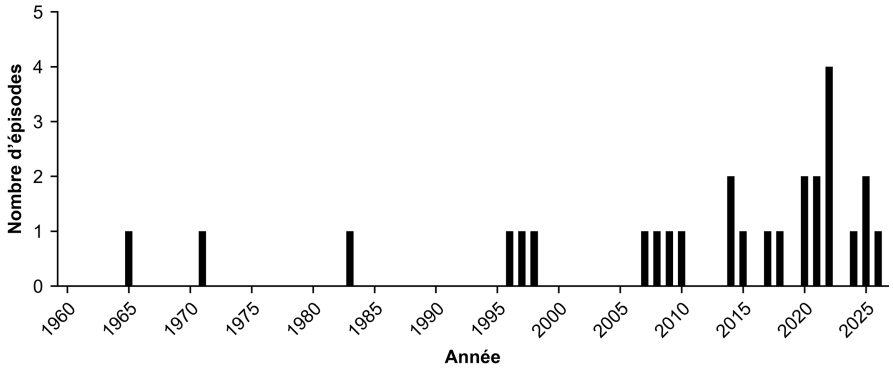



Figure 2. Annual number of flood events, 1960-2026.

By decade, the number of episodes rose from one (1960s to 1980s) to three (1990s and 2000s), then six (2010s), and already twelve in 2020 - 2026 (Figure 3). A Poisson regression on the 67 annual counts confirms a significant increase by a factor of 1.80 per decade (95% CI: 1.38 - 2.35; $p < 0.001$), which remains significant for 1996-2026 alone (factor 1.82; 95% CI: 1.12 - 2.96; $p = 0.016$). The proportion of years with at least one episode rose from 10/54 before 2014 to 10/13 since 2014 (Fisher's exact test, $p < 0.001$).

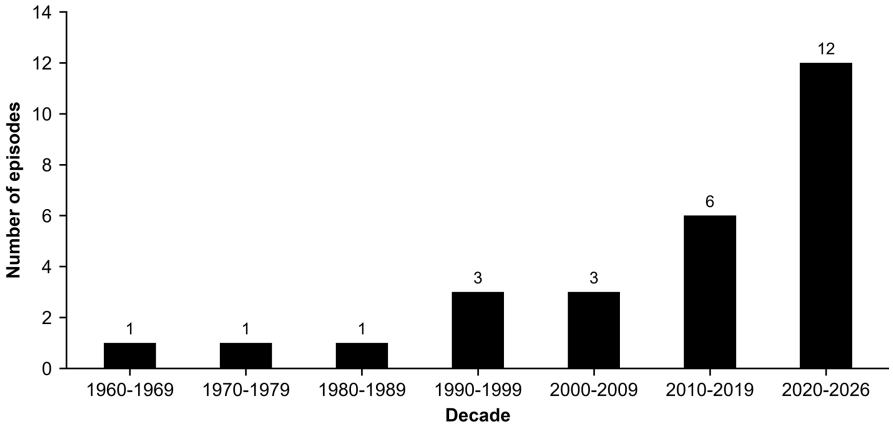



Figure 3. Number of flood events per decade (1960-2026).

## 4.2. Human Impact of Floods from 1960 to 2026

The first three floods (1965, 1971, and 1983) caused no deaths; the first fatalities (28) were recorded in 1996, and 2009 remains the deadliest year, with 40 deaths (Figure 4). Four of the six deadliest years (2014, 2022, 2024, and 2026) occurred after 2013, each with more than 15 deaths.

By decade, deaths rose from 32 in the 1990s to 56 in the 2000s and 85 in the 2010s and already reach 104 in 2020-2026 (Figure 5). The mortality rate rose from 1.19 to 2.12 deaths per million inhabitants per year. Among the affected years, the annual number of deaths increased significantly over time (Spearman's $\rho = 0.59$; $p = 0.006$; $n = 20$).

A seasonal analysis of episodes and deaths reveals a concentration in June. Thus, 77.78% of episodes and 87.36% of deaths occur in the month of June alone

(Table 1). When May and July are included, 88.89% of episodes and 97.47% of deaths are concentrated in the May-July period, the peak of the rainy season in the Abidjan district.

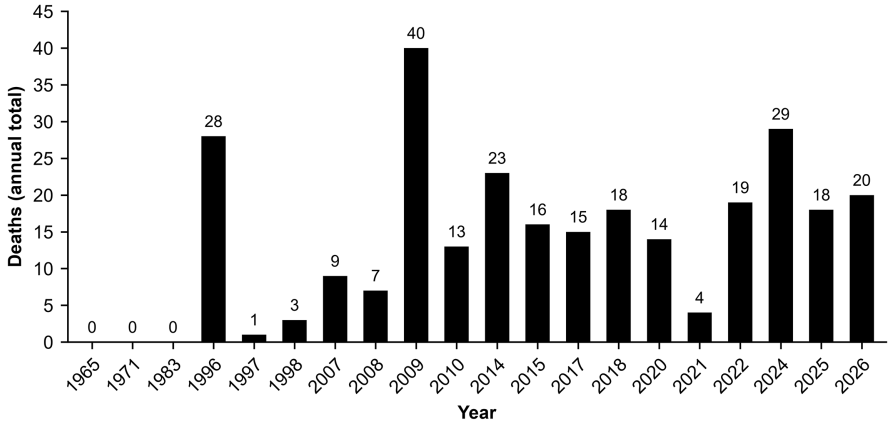



Figure 4. Annual death toll from flooding in Abidjan (1960-2026).

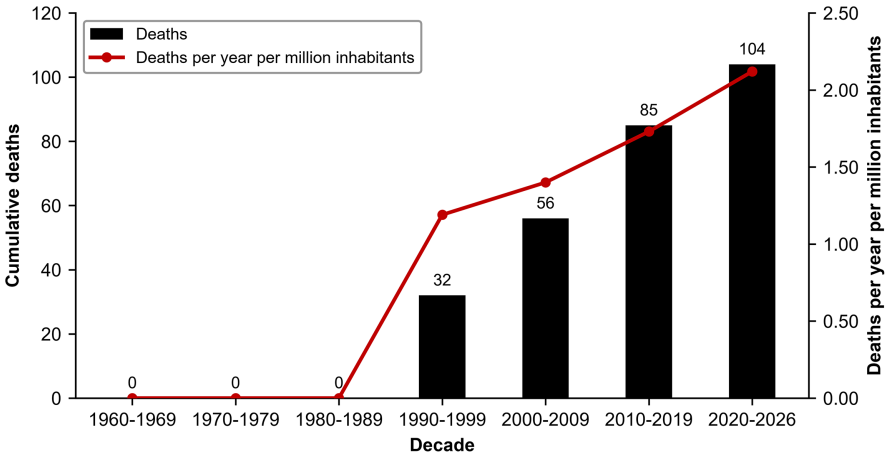



Figure 5. Flood-related deaths per decade (1960-2026).

Table 1. Monthly distribution of flood events and deaths.

| Month of occurrence | Events (%) | Deaths (%) |
|---|---|---|
| May | 7.41 | 10.11 |
| June | 77.78 | 87.36 |
| July | 3.70 | 0 |
| October | 3.70 | 1.44 |
| November | 7.41 | 1.08 |

Furthermore, the two episodes in May (7.41% of episodes and 10.11% of deaths) demonstrate that a small number of events can be particularly deadly. The only episodes recorded outside this period are those in October (3.70% of episodes and 1.44% of deaths) and November (7.41% of episodes and 1.08% of deaths).

### 4.3. Spatial Distribution of Floods

A spatial analysis of the events reveals a highly varied distribution of floods in the Abidjan district between 1960 and June 2026 (Figure 6). Since a single flood can affect multiple municipalities, each episode is counted in every municipality affected.

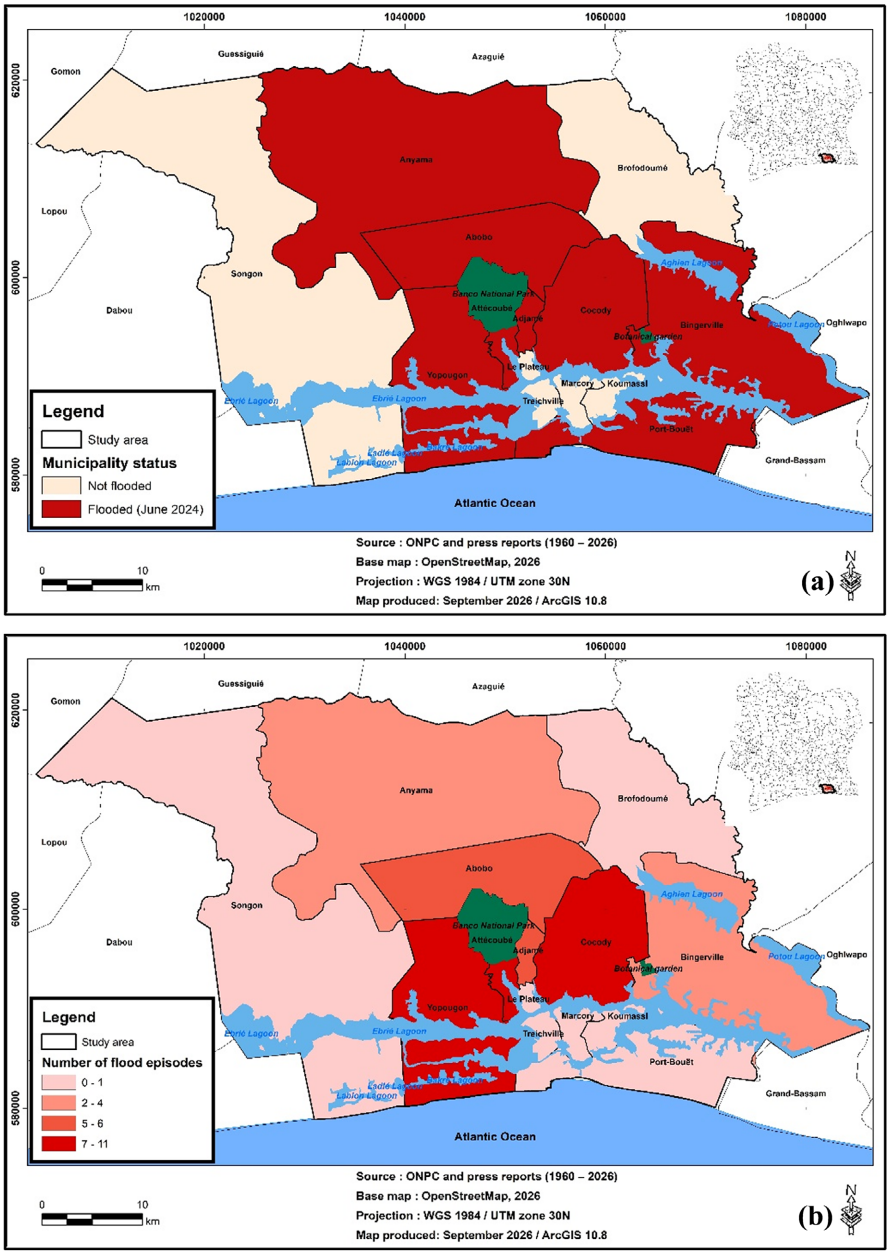



Figure 6. Flood frequency (1960-2026) (a) and municipalities affected by the June 2024 flood (b).

The 23 localized episodes total 54 municipal occurrences, or an average of 2.3 municipalities per episode; 4 episodes could not be localized. Attécoubé (Mossikro, Agban, Kouroukôrô) and Cocody (Riviera, Palmeraie, Deux-Plateaux, Attoban, Gobelet) are the most frequently affected municipalities, each accounting for 11 of

the 27 episodes (40.7%), followed by Yopougon (9 episodes, 33.3%), then Abobo (6), Adjamé (5), Bingerville (4), Anyama (3), and one episode each for Koumassi, Marcory, Plateau, Port-Bouët, and Treichville.

Furthermore, the episode from June 13 to 16, 2024, had the widest spatial extent, affecting eight municipalities (Abobo, Adjamé, Anyama, Attécoubé, Bingerville, Cocody, Port-Bouët, and Yopougon), ahead of the episode of June 14-15, 2025 (seven municipalities), that of October 22, 2021 (four municipalities), and those of June 2009, June 2018, June 2022, and June 2026 (three municipalities each). No event prior to 2009 affected more than two municipalities. However, the trend in the number of municipalities affected per event is not significant (Spearman's $\rho = 0.20$; $p = 0.36$).

### 4.4. Role of Precipitation in the Occurrence of Floods

Precipitation indicators were used to determine whether the increase in the frequency and severity of events reflects more intense precipitation. The indicators for the 20 affected years and the other 47 years are compared in Table 2.

Table 2. Comparison of rainfall indicators between flood years and non-flood years (Welch's t-test and Mann-Whitney U test).

| Indicator | Mean, flood years (n = 20) | Mean, non-flood years (n = 47) | t (Welch) | p (Welch) | p (Mann-Whitney) |
|---|---|---|---|---|---|
| Rx1day (mm) | 81.6 | 51.9 | 2.91 | 0.007 | 0.003 |
| Rx3day (mm) | 114.6 | 79.3 | 3.13 | 0.004 | 0.001 |
| Rx5day (mm) | 133.8 | 101.6 | 2.79 | 0.010 | 0.004 |
| PRCPTOT (mm) | 1 856.1 | 2 021.9 | −2.24 | 0.030 | 0.051 |

The affected years show significantly higher maximum rainfall than the other years. Thus, the average value of Rx1day reaches 81.6 mm in the affected years, compared with 51.9 mm in the other years. A similar trend is observed for Rx3day (114.6 and 79.3 mm) and Rx5day (133.8 and 101.6 mm). Conversely, the annual cumulative precipitation is significantly lower in the affected years (1856.1 mm) than in the other years (2,021.9 mm; Welch's $t = -2.24$; $p = 0.030$). The Mann-Whitney U test confirms these differences for Rx1day ($p = 0.003$), Rx3day ($p = 0.001$), and Rx5day ($p = 0.004$), while the difference in annual cumulative precipitation is only marginal with this test ($p = 0.051$).

Furthermore Table 3 shows that, the Spearman correlation between deaths and rainfall intensity remains weak and nonsignificant, regardless of the indicator ($\rho$ ranging from −0.27 to 0.24; all 95% confidence intervals include zero). With n = 20, only correlations greater than approximately 0.59 could have been detected with 80% power.

Over the period 1960-2025, the Mann-Kendall test indicates a significant increase in Rx1day (+0.37 mm/year; $p = 0.035$) and Rx3day (+0.41 mm/year; $p = 0.048$), while the increase in Rx5day is not significant (+0.38 mm/year; $p = 0.065$).

Annual precipitation exhibits a statistically significant decreasing trend of −7.2 mm/year ($p < 0.001$). This trend remains statistically significant after pre-whitening of the time series, reinforcing the robustness of the result against the effects of temporal autocorrelation.

**Table 3.** Death-rainfall correlations (flood years) and 1960-2025 trends (Spearman correlation; Mann-Kendall test and Sen's slope).

| Test | Variables | Statistic | N | p |
|---|---|---|---|---|
| Correlations with deaths | Rx1day (flood years) | $\rho = 0.22$ | 20 | 0.346 |
| | Rx3day (flood years) | $\rho = 0.23$ | 20 | 0.327 |
| | Rx5day (flood years) | $\rho = 0.24$ | 20 | 0.312 |
| | PRCPTOT (flood years) | $\rho = -0.27$ | 20 | 0.257 |
| Trend 1960-2025 (Mann-Kendall, Sen's slope) | Rx1day | +0.37 mm/an | 66 | 0.035 |
| | Rx3day | +0.41 mm/an | 66 | 0.048 |
| | Rx5day | +0.38 mm/an | 66 | 0.065 |
| | PRCPTOT | −7.2 mm/an | 66 | <0.001 |

Table 4 presents the relationship between maximum daily rainfall, floods, and their human impacts. The annual maximum Rx1day coincides with the day of the flood in only three events (June 11, 1997; June 16, 2022; and June 15, 2025). For the other years, the maximum occurs at another time during the season, sometimes several months before or after the flood. The record for the series, estimated at 181.4 mm, occurred on July 23, 2008, while the flood took place in June. September 26 (97.5 mm) marks the record for 2018, for an event that occurred on the night of June 18 - 19. In 1998, the maximum Rx1day occurred on June 27, while the flood took place on November 16.

**Table 4.** Annual maximum 24-hour rainfall and floods in Abidjan, flood years from 1960 to 2026.

| Year | Rx1day (mm) | Rx1day date | Flood date | Cumulative deaths |
|---|---|---|---|---|
| 1965 | 179.8 | 10/07/1965 | July | 0 |
| 1971 | 89.8 | 13/08/1971 | June | 0 |
| 1983 | 35.5 | 16/06/1983 | June | 0 |
| 1996 | 93 | 15/07/1996 | May 29 | 28 |
| 1997 | 39.2 | 11/06/1997 | June 11 | 1 |
| 1998 | 48.2 | 27/06/1998 | November 16 | 3 |
| 2007 | 30.3 | 19/09/2007 | June | 9 |
| 2008 | 181.4 | 23/07/2008 | June | 7 |
| 2009 | 65.5 | 07/05/2009 | June 11-15 | 40 |

Continued

| | | | | |
|---|---|---|---|---|
| 2010 | 77.2 | 24/09/2010 | June 23-24 | 13 |
| 2014 | 107.4 | 09/05/2014 | June 17 and 19 | 23 |
| 2015 | 91.6 | 05/06/2015 | June 21 | 16 |
| 2017 | 76.8 | 13/06/2017 | June | 15 |
| 2018 | 97.5 | 26/09/2018 | June 18-19 | 18 |
| 2020 | 30.3 | 26/05/2020 | June (2 events) | 14 |
| 2021 | 74.8 | 22/08/2021 | October 22 and November 8 | 4 |
| 2022 | 86.8 | 16/06/2022 | June 6, 16, 21 and 30 | 19 |
| 2024 | 81,6 | 25/06/2024 | June 13-16 | 29 |
| 2025 | 54 | 15/06/2025 | May 21 and June 14-15 | 18 |
| 2026 | 90.6 | 07/06/2026 | June 28-29 | 20 |

Human impact is also not associated with Rx1day (Spearman's $\rho = 0.22$; p = 0.346; n = 20). The three deadliest years 2009 (40 deaths), 2024 (29), and 1996 (28) recorded 65.5 mm, 81.6 mm, and 93.0 mm, respectively, none of which rank among the highest values in the series. Conversely, the two highest Rx1day values, 2008 (181.4 mm) and 1965 (179.8 mm), corresponded to 7 deaths and 0 deaths, respectively. The years 2007 and 2020 had the lowest Rx1day values among the affected years (30.3 mm), but recorded 9 and 14 deaths, respectively.

### 4.5. Rainfall on Flood Days and the Reliability of ERA5

For the 19 episodes with precisely determined dates, ERA5 rainfall on flood days was generally modest. P1d ranged from 1.8 to 86.8 mm (median 15.0 mm) and P3d from 4.3 to 101.4 mm (median 27.5 mm) (Table 5). Regardless of the time frame considered, most floods correspond to rainfall events that occur, on average, more than once every two years. This is the case for 17 out of 19 floods based on daily rainfall, 16 based on the 3-day total, and 17 based on the 5-day total. Only three episodes reach or exceed a 2-year return period. June 18 and 19, 2018; June 14 and 15, 2025; and, most notably, June 16, 2022 for which the daily rainfall (86.8 mm) occurs on average about once every five years. No ERA5 rainfall on a flood day reaches a 10-year return period. Finally, these rainfall events are not linked to human casualties: the years in which ERA5 indicates the heaviest rainfall are not the deadliest (P1d: $\rho = -0.18$, p = 0.55; P3d: $\rho = -0.09$, p = 0.78; P5d: $\rho = 0.14$, p = 0.65; n = 13).

These low values do not mean that flooding occurs with modest rainfall. Rather, they reflect a limitation of the ERA5 model. Each value is an average over a grid cell approximately 28 km on a side, within which a violent but localized thunderstorm is significantly "diluted." The airport weather station confirms this (Table 6). During the three years for which complete data are available (2023 to 2025),

its highest daily rainfall amounts were 4 to 28 times greater than those of ERA5 on the same days. On June 15, 2025, the day of the flood, it recorded 302.5 mm, compared to 54.0 mm in ERA5.

The ORIESA network confirms this underestimation over a much larger sample. Between June 2015 and June 2023 (2933 days with at least three operational rain gauges), ERA5 accurately reproduces the network's average daily rainfall (5.0 vs. 5.3 mm/day), but poorly captures its day-to-day variability (r = 0.46). On the 44 days when at least one rain gauge recorded more than 100 mm, ERA5 showed a median of only 12.9 mm and exceeded 50 mm in only three days. The median annual maximum at the rain gauges (117.8 mm) is 1.8 times the ERA5 Rx1day value for the same year, and on the day of each annual maximum recorded by the rain gauges, the ERA5 showed a median of 13.6 mm.

**Table 5.** ERA5 rainfall on dated flood days and return period of 3-day rainfall totals (Gumbel distribution fitted to 1960-2025 annual maxima).

| Flood date | Daily rainfall (P1d) | | 3-day total (P3d) | | 5-day total (P5d) | | Deaths in year |
|---|---|---|---|---|---|---|---|
| | Rainfall (mm) | Return period (years) | Rainfall (mm) | Return period (years) | Rainfall (mm) | Return period (years) | |
| May 29, 1996 | 11.4 | <2 | 24.5 | <2 | 33.1 | <2 | 28 |
| June 11, 1997 | 39.2 | <2 | 54.6 | <2 | 58.5 | <2 | 1 |
| November 16, 1998 | 18.2 | <2 | 44.9 | <2 | 47.8 | <2 | 3 |
| June 11-15 2009 | 16.1 | <2 | 37.1 | <2 | 59.8 | <2 | 40 |
| June 23-24, 2010 | 15 | <2 | 27.5 | <2 | 41.3 | <2 | 13 |
| June 17, 2014 | 1.8 | <2 | 4.3 | <2 | 43.3 | <2 | 23 |
| June 19, 2014 | 7.5 | <2 | 25.3 | <2 | 27.8 | <2 | |
| June 21, 2015 | 4.6 | <2 | 9.3 | <2 | 19.3 | <2 | 16 |
| June 18-19, 2018 | 59 | 2.2 | 92.2 | 2.5 | 100.6 | <2 | 18 |
| October 22, 2021 | 13.6 | <2 | 21.6 | <2 | 28.8 | <2 | 4 |
| November 8, 2021 | 7.6 | <2 | 18.4 | <2 | 30.5 | <2 | |
| June 6, 2022 | 21.1 | <2 | 33.2 | <2 | 40.6 | <2 | 19 |
| June 16, 2022 | 86.8 | 5.1 | 101.4 | 3.2 | 114.5 | 2.6 | |
| June 21, 2022 | 8.6 | <2 | 25.3 | <2 | 39.2 | <2 | |
| June 30, 2022 | 22.5 | <2 | 32.5 | <2 | 44.9 | <2 | |
| June 13-16, 2024 | 17.1 | <2 | 43.6 | <2 | 52.5 | <2 | 29 |
| Mai 21, 2025 | 10.2 | <2 | 13.8 | <2 | 57.2 | <2 | 18 |
| June 14-15, 2025 | 5 | 2 | 86.3 | 2.2 | 108.8 | 2.2 | |
| June 28-29, 2026 | 10.1 | <2 | 27.5 | <2 | 37.5 | <2 | 20 |

Table 6. Comparison between ground-measured rainfall and ERA5 rainfall.

| Indicator | Ground measurement (mm) | ERA5 (mm) | Ratio |
|---|---|---|---|
| **Airport station (WMO 65578), 2023-2025** | | | |
| 11 June 2023 (annual maximum) | 130.3 | 30.4 | 4.3 |
| 20 June 2024 (annual maximum) | 161.4 | 5.7 | 28.3 |
| 15 June 2025 (annual maximum, flood day) | 302.5 | 54 | 5.6 |
| **ORIESA network, 2015-2023** | | | |
| Mean daily rainfall (network average) | 5.3 | 5 | 1.1 |
| Days with ≥ 1 gauge exceeding 100 mm (44 days): median rainfall at the wettest gauge | 128 | 12.9 | 9.9 |
| Number of these 44 days with ERA5 exceeding 50 mm | — | 3 | — |
| Annual maximum, regardless of day (medians, 42 gauge-years) | 117.8 | 74.8 | 1.6 |
| Gauge annual maximum and ERA5 rainfall on the same day (medians) | 117.8 | 13.6 | 8.7 |

On days when flooding occurred, the discrepancy between rain gauges and ERA5 was even more pronounced (Table 7). Of the eight flood events covered by the network, six recorded more than 100 mm at least one rain gauge.

Table 7. Daily rainfall on dated flood days: ORIESA rain gauges and ERA5 (maximum over the flood day(s) and the preceding day).

| Flood or rainfall class | Gauge in operation | Wettest gauge | Wettest gauge rainfall (mm) | Gauge median (mm) | ERA5 (mm) | Ratio |
|---|---|---|---|---|---|---|
| **Dated flood days** | | | | | | |
| June 21, 2015 | 3 | Achokoi | 2.5 | 2.4 | 4.6 | 0.5 |
| June 18-19, 2018 | 5 | Achokoi | 151.9 | 133.7 | 59.0 | 2.6 |
| October 22, 2021 | 18 | Brofodoumé | 102.0 | 21.5 | 13.6 | 7.5 |
| November 8, 2021 | 17 | Riviera Nord F9 | 121.0 | 30.5 | 9.5 | 12.7 |
| June 6, 2022 | 19 | Attiekoi CET | 7.8 | 0.5 | 21.1 | 0.4 |
| June 16, 2022 | 18 | Adiopodoumé F1 | 147.5 | 91.5 | 86.8 | 1.7 |
| June 21, 2022 | 19 | Cité Sir | 329.3 | 172.7 | 15.6 | 21.1 |
| June 30, 2022 | 19 | Marcory | 187.1 | 58.5 | 22.5 | 8.3 |
| **All rainy days, June 2015-June 2023 (median values)** | | | | | | |
| Days with 1 - 20 mm (1077 days; ERA5 lower on 59% of days) | 13 | — | 5.0 | 0.5 | 3.2 | 1.4 |
| Days with 20 - 50 mm (429 days; ERA5 lower on 99% of days) | 15 | — | 30.5 | 7.0 | 6.6 | 4.7 |

**Continued**

| | | | | | | |
|---|---|---|---|---|---|---|
| Days with 50 - 100 mm (180 days; ERA5 lower on 99% of days) | 14 | — | 66.0 | 22.0 | 9.7 | 7.0 |
| Days with 100 - 200 mm (41 days; ERA5 lower on 100% of days) | 15 | — | 125.0 | 52.0 | 13.5 | 9.0 |
| Days with > 200 mm (3 days; ERA5 lower on 100% of days) | 18 | — | 231.1 | 22.8 | 8.6 | 38.3 |

The most striking example is June 21, 2022: 329.3 mm at the rain gauge that recorded the highest rainfall (Cité Sir), and a median of 172.7 mm across the 19 rain gauges, compared to 15.6 mm in the ERA5. Only two floods on June 21, 2015, and June 6, 2022 did not correspond to any recorded heavy rainfall; in 2015, only three rain gauges, located on the outskirts of the district, were operational.

These thunderstorms are highly localized. On days when one rain gauge recorded more than 50 mm, 40% of the other rain gauges recorded less than 20 mm, and the least affected gauge recorded almost nothing (a median of 2.4 mm). Two rain gauges less than 5 km apart record very similar rainfall amounts, but this similarity decreases significantly beyond 10 km. A thunderstorm can therefore flood a few neighborhoods without being detected in the rest of the district or in the ERA5. Table 7 shows that this underestimation increases with the intensity of the thunderstorm. The median ratio between ground-level rainfall and ERA5 ranges from 1.4 for rainfall amounts under 20 mm to 4.7 between 20 and 50 mm, and then to 9.0 between 100 and 200 mm. As soon as the rain gauge with the highest rainfall exceeds 20 mm, ERA5 indicates less rainfall than that gauge on almost every day (99 to 100 percent of the time).

## 5. Discussion

This study highlights an increase in flooding and associated deaths in the Abidjan district between 1960 and June 2026, with near-annual events since 2014 and often multiple events during a single season. This trend is consistent with the continental trend documented by [16], who, using the EM-DAT database from 1927 to 2020, demonstrated a significant increase in the frequency of floods and flood-related deaths across all African regional economic communities. Similarly, [17], based on an analysis of mortality trends in EM-DAT, showed that Africa is the only major region in the world where the frequency of deadly floods has increased since the late 1980s.

Over the period 1960-2025, the Rx1day and Rx3day indices show a statistically significant upward trend, while Rx5day shows a smaller, non-significant increase. This result is consistent with previous studies conducted along the Ivorian coast and in the Abidjan district. [18], using daily data from 1971 to 2022, showed that extreme daily rainfall accounts for a growing proportion of coastal flooding. Indeed, an increased frequency of intense daily rainfall is likely to exceed the capacity of drainage systems [19]. Finally, this finding is consistent with the IPCC's as-

sessment for West Africa, which reports an intensification of observed extreme precipitation [20].

However, no significant correlation appears between precipitation indices and the severity of the recorded floods. This lack of a significant association should be interpreted with caution: with 20 affected years, only correlations greater than approximately 0.59 could be detected with 80% power, and the annual maximum rainfall often occurred on a different day than the flood. Ground-based rainfall data help to partially resolve this uncertainty. Most of the floods covered by the ORIESA network coincided with thunderstorms producing 100 to 330 mm of rainfall at least one rain gauge, which ERA5 modeled as ordinary rainfall. Flooding in Abidjan is therefore triggered by intense rainfall, but by thunderstorms so localized that a single reanalysis grid point or even a single station cannot adequately represent them. The lack of correlation between ERA5 rainfall and fatalities thus reflects the limitations of the rainfall data rather than an absence of rainfall's effect. This interpretation aligns with the conclusion of [21], based on the longest available rainfall series for the city, which states that the worsening of urban flooding in Abidjan is due more to urbanization and drainage problems than to an increase in rainfall intensity. It is also consistent with the continental analyses by [22], who attribute most of the increase in damage and mortality to increased exposure rather than to an increase in the hazard itself.

Comparing with station data has broader implications. Reanalyzes such as ERA5 are increasingly used to study flood risk in African cities with limited data, but at a resolution of 0.25˚, they cannot reproduce the brief, localized convective storms that cause urban flash floods. In Abidjan, thunderstorms that recorded 150 to 330 mm on rain gauges appeared as rainfall amounts of 15 to 59 mm in ERA5. Studies of the triggers of urban flooding based solely on reanalyses therefore risk incorrectly concluding that floods occur during ordinary rainfall events. Dense rain gauge networks, such as the one operating in Abidjan since 2015 [21], are essential in this regard.

The risk assessments available for the district supports this interpretation. The multi-criteria mapping by [1] attributes flood risk as much to population density and urban structure as to rainfall variability. Studies conducted in Bingerville [23] and across the entire district [24] identify rapid urbanization, undersized drainage infrastructure, and the encroachment on stormwater basins as key factors. The government report on the June 2018 floods [8] had already described damage concentrated in a small number of structurally vulnerable neighborhoods. This context sheds light on the main finding of our analysis: the recurrence of the same municipalities (Attécoubé, Cocody, Yopougon, Abobo) from one event to the next does not appear to be coincidental, but rather stems from physical characteristics (low-lying areas, steep slopes, lagoon outlets) and socioeconomic factors (settlement in high-risk areas, precarious housing) that persist over time.

The increase in the number of recorded events must, however, be viewed in context. Before 1996, only one event per year was reported, and media coverage

has improved significantly since then; part of this trend may therefore reflect improved data collection, even though the increase in the number of events remains significant for the period 1996-2026 alone (Poisson regression: factor of 1.82 per decade; $p = 0.016$). Similarly, when considered relative to the population which more than sextupled between 1975 and 2021 mortality is increasing much more slowly than the crude number of deaths (+78% per million inhabitants versus +364% for the average annual number of deaths that is, 3.2 versus 14.9 deaths per year, between the 1990s and 2020-2026). The rise in the human toll is therefore primarily due to the increased frequency of events and the growth of the exposed population.

The high seasonal concentration of deaths between May and July (97.47%), with 87.36% occurring in June alone, confirms the finding by [21], who found that virtually all floods in Abidjan occur during the main rainy season. This is consistent with the seasonality of convective systems in the Gulf of Guinea and with IPCC projections of more intense rainfall events during the peak of the season [20]. From an operational standpoint, this concentration provides a direct opportunity for action: preventive measures (cleaning drainage systems, activating early-warning systems, targeted awareness campaigns) can be planned within a narrow window leading up to June.

Several limitations should be noted. The flood inventory relies on official reports and news media, which underestimate minor events, particularly prior to 1996. At its 0.25˚ resolution, ERA5 smooths out local convective rainfall and likely underestimates point-specific intensities, as shown by the comparison with the ORIESA network and the airport station; ground-based rainfall data cover only eight of the 27 episodes. Annual rainfall rarely coincides with flood days (three out of 20 cases), so annual indices provide only an imperfect representation of the rainfall that triggered each event. Finally, urbanization was not directly quantified in this study; its role is inferred from the spatial recurrence of floods, population growth, and previous risk assessments [1] [23] [24]. Longer ground-based rainfall time series covering all floods, as well as indicators of built-up areas, would help overcome these limitations in future studies.

## 6. Conclusions

This reconstruction of the flood history in Abidjan from 1960 to 2026 highlights a statistically significant increase in the number of damaging floods (a 1.8-fold increase per decade; Poisson regression, $p < 0.001$), which persists over the better-documented period from 1996 to 2026. Floods have been reported in 10 out of 13 years since 2014, often involving multiple episodes (Fisher's exact test, $p < 0.001$), and the death toll for the period 2020 - 2026 (104 deaths) already exceeds that of each of the preceding decades. This trend is not explained by rainfall as represented by ERA5, whose annual and event-based values show no significant correlation with mortality. However, ground-based rainfall data show that ERA5 does not capture the intense, localized thunderstorms often ranging from 100 to 330

mm at a rain gauge that trigger most floods. The rise in the human death toll is more consistent with rapid and largely uncontrolled urbanization, which concentrates exposure in a small number of structurally vulnerable municipalities (Attécoubé, Cocody, Yopougon, Abobo). However, a contribution from climate change cannot be ruled out: annual maximum rainfall over 1 and 3 days (Rx1day, Rx3day) increased significantly between 1960 and 2025. Three key areas emerge for risk management:

- a harmonized and centralized system for post-disaster data collection that systematically covers deaths, injuries, missing persons, and property damage, a prerequisite for reliable long-term statistical monitoring, supplemented by making SODEXAM's daily and sub-daily rainfall data available to researchers, as reanalyzes cannot capture the local thunderstorms that trigger urban flooding;
- accelerating relocation programs in mapped high-risk areas, particularly in Attécoubé, with housing solutions rather than mere demolitions;
- strengthening and regularly maintaining drainage systems in the most vulnerable municipalities so that they can handle heavy rainfall and focus early-warning efforts on the June risk window during which nearly all recorded events occur by relying on locally measured rainfall thresholds and maps of vulnerable sites rather than a single threshold.

## Acknowledgements

The authors thank the ORIESA observatory and its data producers (E. Zahiri, L. Séguis and colleagues) for making the Abidjan rainfall data openly available.

## Data Availability

The flood inventory compiled for this study is available from the corresponding author upon reasonable request. ERA5 data are freely available from the Copernicus Climate Change Service Climate Data Store (https://doi.org/10.24381/cds.adbb2d47) and were extracted via the Open-Meteo archive (https://open-meteo.com/en/docs/historical-weather-api). Daily records from the Abidjan Airport station (WMO 65578) were obtained from Meteostat (https://meteostat.net/en/station/65578). ORIESA rainfall data are available from the DataSuds repository (https://doi.org/10.23708/AN9SKZ) under a CC BY-NC 4.0 license.

## Author Contributions

Conceptualization, K.M.K. and N.H.M.; methodology, K.M.K.; software, K.M.K.; validation, K.M.K. and N.H.M.; formal analysis, K.M.K.; investigation, K.M.K.; resources, K.M.K. and N.H.M.; data curation, K.M.K.; writing—original draft preparation, K.M.K.; writing—review and editing, K.M.K. and N.H.M.; visualization, K.M.K.; supervision, N.H.M.; project administration, K.M.K. All authors have read and agreed to the published version of the manuscript.

## Conflicts of Interest

The authors declare no conflicts of interest.

## References


[1] Danumah, J.H., Odai, S.N., Saley, B.M., Szarzynski, J., Thiel, M., Kwaku, A., *et al.* (2016) Flood Risk Assessment and Mapping in Abidjan District Using Multi-Criteria Analysis (AHP) Model and Geoinformation Techniques, (Cote d'Ivoire). *Geoenvironmental Disasters*, **3**, Article No. 10. https://doi.org/10.1186/s40677-016-0044-y

[2] Mahé, G. (2006) Variabilité pluie-débit en Afrique de l'Ouest et Centrale au 20e siècle: Changements hydroclimatiques, occupation du sol et modélisation hydrologique. Ph.D. Thesis, Université Montpellier 2. https://www.documentation.ird.fr/hor/fdi:010043107

[3] Tie, A.G.B., Konan, B., Brou, Y.T., Issiaka, S., Fadika, V. and Srohourou, B. (2007) Estimation des pluies exceptionnelles journalières en zone tropicale: Cas de la Côte d'Ivoire par comparaison des lois lognormale et de Gumbel. *Hydrological Sciences Journal*, **52**, 49-67. https://doi.org/10.1623/hysj.52.1.49

[4] Gumbel, E.J. (1958) Statistics of Extremes. Columbia University Press. https://doi.org/10.7312/gumb92958

[5] Danumah, J.H., Ataba, W.A., Jofack Sokeng, V.C., Akpa, Y.L., Saley, M.B. and Ogilvie, A. (2026) Assessing Urban Flood Susceptibility Using Random Forest Machine Learning and Geospatial Technologies: Application to the Bonoumin-Palmeraie Watershed, Abidjan (Côte d'Ivoire). *Water*, **18**, Article 402. https://doi.org/10.3390/w18030402

[6] Kouassi, K.M. (2022) Estimation des extrêmes hydropluviométriques à partir de l'analyse fréquentielle et cartographie des risques d'inondation sur la portion ivoirienne du bassin versant de la rivière Bia. Thèse de doctorat, Université Félix Houphouët-Boigny, 218 p.

[7] Saley, M.B., Kouamé, F.K., Penven, M.J., Biémi, J. and Kouadio, H.B. (2005) Cartographie des zones à risque d'inondation dans la région semi-montagneuse à l'ouest de la Côte d'Ivoire: Apports des MNA et de l'imagerie satellitaire. *Télédétection*, **5**, 53-67.

[8] République de Côte d'Ivoire (2019) Évaluation des pertes, dommages et besoins suite aux inondations de juin 2018 à Abidjan [Rapport gouvernemental].

[9] Hersbach, H., Bell, B., Berrisford, P., Hirahara, S., Horányi, A., Muñoz-Sabater, J., *et al.* (2020) The ERA5 Global Reanalysis. *Quarterly Journal of the Royal Meteorological Society*, **146**, 1999-2049. https://doi.org/10.1002/qj.3803

[10] Zahiri, E., Séguis, L., Kacou, M., Kamagaté, B., Dao, A., Perrin, J.L., Koffi, S.E., Guilliod, M. and Dutremble, C. (2023) Daily Rainfall in Abidjan District (Côte d'Ivoire) (2015-) (Version 8) [Data Set]. https://doi.org/10.23708/AN9SKZ

[11] Institut National de la Statistique (INS) (2021) Recensements généraux de la population et de l'habitat (RGPH) de 1975, 1988, 1998, 2014 et 2021. INS.

[12] Kendall, M.G. (1975) Rank Correlation Methods. 4th Edition, Charles Griffin.

[13] Mann, H.B. (1945) Nonparametric Tests against Trend. *Econometrica*, **13**, 245-259. https://doi.org/10.2307/1907187

[14] Sen, P.K. (1968) Estimates of the Regression Coefficient Based on Kendall's Tau. *Journal of the American Statistical Association*, **63**, 1379-1389. https://doi.org/10.1080/01621459.1968.10480934

[15] Yue, S., Pilon, P., Phinney, B. and Cavadias, G. (2002) The Influence of Autocorrelation on the Ability to Detect Trend in Hydrological Series. *Hydrological Processes*, **16**, 1807-1829. https://doi.org/10.1002/hyp.1095

[16] Houteta, D.K., Sylla, M.B., Tall, M., Dajuma, A., Pal, J.S., Lennard, C., *et al.* (2025) Spatial and Temporal Trend Analysis of Flood Events across Africa during the Historical Period. *Water*, **17**, Article 3531. https://doi.org/10.3390/w17243531

[17] Cael, B.B. (2025) Climate Hazard Mortality: Diagnosing Trends and Outliers. *Geophysical Research Letters*, **52**, e2025GL119218. https://doi.org/10.1029/2025gl119218

[18] Coulibaly, K.A., N'Da, K.C., Sylla, D., Dibi-Anoh, P.A. and Goula, B.T.A. (2024) Persistance des séquences pluvieuses et risques d'inondations de 1971 à 2022 en Côte d'Ivoire. *European Scientific Journal*, *ESJ*, **20**, 53. https://doi.org/10.19044/esj.2024.v20n9p53

[19] Konaté, L., Kouadio, B.H., Djê, B.K., Aké, G.E., N'Guessan, B.V.H., Gnagne, L., Kouamé, E.K. and Biémi, J. (2016) Caractérisation des pluies journalières intenses et récurrences des inondations: Apport des totaux glissants trois jours à la détermination d'une quantité seuil d'inondation. *International Journal of Innovation and Applied Studies*, **17**, 990-1003.

[20] Intergovernmental Panel on Climate Change (IPCC) (2023) Climate Change 2021—The Physical Science Basis. Cambridge University Press. https://doi.org/10.1017/9781009157896

[21] Yao, C., Kacou, M., Koffi, E.S., Dao, A., Dutremble, C., Guilliod, M., *et al.* (2024) Rainfall Risk over the City of Abidjan (Côte d'Ivoire): First Contribution of the Joint Analysis of Daily Rainfall from a Historical Record and a Recent Network of Rain Gauges. *Proceedings of IAHS*, **385**, 259-265. https://doi.org/10.5194/piahs-385-259-2024

[22] Di Baldassarre, G., Montanari, A., Lins, H., Koutsoyiannis, D., Brandimarte, L. and Blöschl, G. (2010) Flood Fatalities in Africa: From Diagnosis to Mitigation. *Geophysical Research Letters*, **37**, L22402. https://doi.org/10.1029/2010gl045467

[23] Eba, A.E.L., Ake, G.E., Gouadou, D.F. and Jourda, J. (2021) Évaluation de la vulnérabilité à l'inondation des communes à proximité des grandes villes ouest-africaines: Cas de la commune de Bingerville. *European Scientific Journal*, *ESJ*, **17**, 277. https://doi.org/10.19044/esj.2021.v17n14p277

[24] Traoré, K. (2023) Évaluation du risque d'inondation par intégration du SAGA Wetness Index (SAGAWI) et de l'analyse hiérarchique des procédés (AHP): Cas du District autonome d'Abidjan. *Belgeo*, No. 1, 23 p. https://doi.org/10.4000/belgeo.60310